Photoconversion of carbon dioxide in zinc–copper–gallium layered double hydroxides: The kinetics to hydrogen carbonate and further to CO/methanol

Motoharu Morikawa [a,1], Naveed Ahmed [b,1], Yusuke Yoshida [b], Yasuo Izumi [b,*]

[a] Department of Nanomaterial Science, Graduate School of Advanced Integration Science, Chiba University, Yayoi 1-33, Inage-ku, Chiba 263-8522, Japan
[b] Department of Chemistry, Graduate School of Science, Chiba University, Yayoi 1-33, Inage-ku, Chiba 263-8522, Japan

ARTICLE INFO

ABSTRACT

Photocatalytic reaction mechanism for the conversion of CO_2 into methanol and CO using layered double hydroxides (LDHs) consisting of Zn, Cu, and Ga was investigated. X-ray absorption fine structure was applied to determine the LDH site structures and to monitor the diffusion of photogenerated electrons to Cu^{II} sites. Electron diffusion to Cu sites was an order of magnitude faster in the direction of the cationic layers ($580\ \mu mol\ h^{-1}\ g_{cat}^{-1}$) than in the perpendicular direction. According to Fourier-transform infrared spectroscopy, CO_2 was in equilibrium with hydrogen carbonate ($1629\ cm^{-1}$ for $H^{13}CO_3$) for the reaction with hydroxy group from the cationic layer or interlayer site and/or with interlayer water. The equilibrium reactions were faster for $[Zn_3Ga(OH)_8]^+{}_2[Cu(OH)_4]^{2-}\cdot mH_2O$ ($400–110\ \mu mol\ h^{-1}\ g_{cat}^{-1}$) than for $[Zn_{1.5}Cu_{1.5}Ga(OH)_8]^+{}_2(CO_3)^{2-}\cdot mH_2O$. Furthermore, the reductive decomposition of hydrogen carbonate was suggested in H_2 under UV–visible light, suggesting photocatalytic pathway to methanol/CO.

© 2013 Elsevier B.V. All rights reserved.

1. Introduction

Carbon dioxide is one of the major greenhouse gases, and methods to reduce its concentration in the atmosphere require urgent attention [1–10]. It is advantageous to capture CO_2 from the atmosphere or factories/power stations and convert it to fuel using a sustainable source of energy such as sunlight. This option simultaneously solves the problems of global warming and sustainable energy shortage. Recently, many investigators have researched this topic; however, more efficient, inexpensive photocatalyst needs to be developed to achieve its practical application [2–4,8–10].

In this regard, a study of selective CO_2 photoconversion to methanol (68 mol%) was reported using H_2 and layered double hydroxides (LDHs) of $[Zn_{1.5}Cu_{1.5}Ga^{III}(OH)_8]^+{}_2(CO_3)^{2-}\cdot mH_2O$ [11]. The inclusion of Cu ions in the cationic layers of the photocatalysts improved the selectivity for methanol formation compared to CO formation. The substitution of interlayer carbonate anions for $[Cu(OH)_4]^{2-}$ anions further boosted the methanol selectivity to 88 mol% [12]. The conversion rate was higher by 3.1 times using $[Zn_{1.5}Cu_{1.5}Al^{III}(OH)_8]^+{}_2(CO_3)^{2-}\cdot mH_2O$ than that using $[Zn_{1.5}Cu_{1.5}Ga(OH)_8]^+{}_2(CO_3)^{2-}\cdot mH_2O$, but the Al analogue was more selective to CO formation (74%) [11].

Photoreduction of CO_2 to CO with water was also reported using LDH compounds, for example, $[Ni_3In(OH)_8]^+{}_2(CO_3)^{2-}\cdot mH_2O$ and $[Ni_3Ga(OH)_8]^+{}_2(CO_3)^{2-}\cdot mH_2O$ [13] or the combination of $[Zn_{1.5}Cu_{1.5}Ga(OH)_8]^+{}_2(CO_3)^{2-}\cdot mH_2O$ and WO_3 (or TiO_2) separated by proton-conducting film [14].

Studies of CO_2 photoreduction have been intensively published [8,15,16]. In the case of CO_2 photoreduction using LDHs, it also needs to be investigated that the CO_2 conversion to fuels proceeded photocatalytically rather than thermally for the intrinsic storage of solar energy as fuels [8]. It is also important to monitor the surface species derived from CO_2 under the photocatalytic reaction conditions [15,16]. Furthermore, the photocatalytic reaction mechanism has rarely been clarified except for a few examples using TiO_2, which include a mechanistic study of formic acid formation from supercritical CO_2 based on electron spin resonance (ESR) [17,18], another study describing methane formation from gaseous CO_2 and H_2O based on ESR [19], and an unexpected result from an ESR- and density functional theory (DFT) calculations-based investigation describing methane formation via C_2-glyoxal (OHC—CHO) [20].

In this paper, an investigation of the site structure for a LDH $[Zn_3Ga(OH)_8]^+{}_2[Cu(OH)_4]^{2-}\cdot mH_2O$ as semiconductor photocatalyst used in the conversion of CO_2 to hydrogen carbonate under light irradiation was performed by extended X-ray absorption fine structure (EXAFS). The kinetics of the conversion to hydrogen carbonate, initiated by charge separation in the LDH compounds under UV–visible light, was investigated in detail by X-ray absorption

near-edge structure (XANES) and Fourier-transform infrared (FTIR) spectroscopy [21,22]. The relevance to the photocatalytic conversion of CO_2 into methanol is discussed.

2. Experimental

The LDH compound with the formula $[Zn_{1.5}Cu_{1.5}Ga(OH)_8]^+_2(CO_3)^{2-} \cdot mH_2O$ was synthesized from an aqueous solution of metal nitrates and sodium carbonate at a controlled pH (pH 8). Details of the synthetic procedure were described in Ref. [11]. LDH compounds with the formula $[Zn_{3-x}Cu_xGa(OH)_8]^+_2[Cu(OH)_4]^{2-} \cdot mH_2O$ ($x = 0$, 1.5) were synthesized from an aqueous solution of metal nitrates and ammonium tetrachlorocuprate dihydrate at the same pH (pH 8). The details of this procedure were described in Ref. [12].

The obtained precipitates were filtered using a membrane filter, washed with deionized water, and dried in ambient air at 290 K for 5 days. The purity of the deionized water used in the experiments was <0.06 μS cm^{-1}. No C-containing chemicals were used except for Na_2CO_3 for these LDH syntheses. For the latter LDH compounds, all synthetic steps up to the filtration and washing (water) of the LDHs were performed in an argon atmosphere.

The photocatalysts were evacuated (10^{-6} Pa) at 290 K for 2 h prior to kinetic tests. Photocatalytic CO_2 reduction tests and control tests in the dark were performed in a closed circulating system under CO_2 at 0.20–2.1 kPa and H_2 at 21.7 kPa using a quartz cell illuminated by a 500-W xenon arc lamp (Ushio, Model UI-502Q; 42 mW cm^{-2}) [23]. The distance between the lamp exit window and the bottom of the cell was 20 mm. The products were analyzed using an inline gas chromatograph equipped with a thermal conductivity detector (GC-TCD; Shimadzu, Model GC-8A). The details are described in Refs. [11,12].

In situ XANES measurements were conducted in a transmission mode at the Photon Factory on beamline 7C (KEK, Tsukuba) and at SPring-8 on beamline 01B1 (Ako) [24] for Cu, Zn, or Ga in LDHs. An LDH photocatalyst disk (ϕ = 2 cm) was set in an air-tight quartz batch cell equipped with polyethylene naphthalate windows (Q51-16, Teijin) [25,26] under CO_2 at 2.1 kPa and H_2 at 21.7 kPa and irradiation by UV–visible light from a 500-W xenon arc lamp (UI-502Q). The distance between the lamp exit window and the sample disk was 20 mm. The light intensity was 42 mW cm^{-2} at the sample position.

The EXAFS measurements were also conducted in a transmission mode for LDH photocatalyst powder pretreated in vacuum (10^{-6} Pa) at 290 K for 2 h. Data analysis software XDAP version 2.2.7 (XAFS Services International, Woudenberg, the Netherlands) was used. EXAFS spectra were also generated theoretically using ab initio multiple scattering calculation code FEFF version 8.4 [27] for comparison to the experimental spectra.

The surface species over a 2-cm-ϕ self-supporting pressed LDH disk (50 mg) placed under a CO_2 atmosphere in a quartz photoreaction cell [28] equipped with NaCl windows on both sides was monitored by an FTIR instrument (JASCO, Model FT/IR-4200) equipped with a mercury–cadmium–tellurium-M detector. The LDH sample disk was evacuated (10^{-6} Pa) at 290 K for 2 h prior to taking spectral measurements. The spectrum acquired for each freshly evacuated sample was set as a reference spectrum. The energy resolution was set to 2 cm^{-1}. The in situ FTIR measurements were basically performed at 290 K. The sample was irradiated by UV–visible light from a 500-W xenon arc lamp (Ushio, Model SX-UID502XAM) via quartz fiber light guide (San-ei Electric Co., Model 5ϕ-2B-1000L; the length: 1075 mm). The distance between the fiber light exit and sample disk was 90 mm. The light intensity at the sample position was 88 mW cm^{-2}. During illumination, the temperature of sample reached as high as 310 K. The
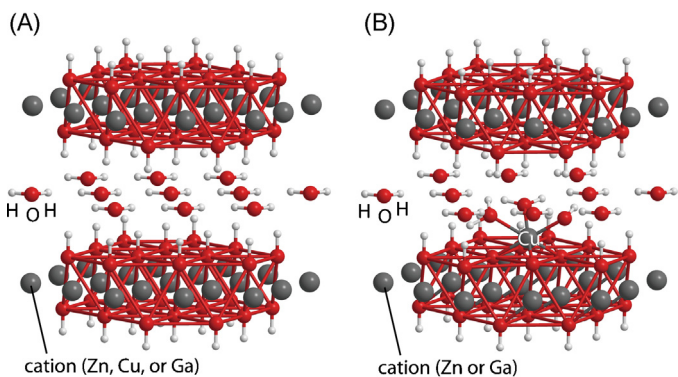

Fig. 1. Structure of $[Zn_{3-x}Cu_xGa(OH)_8]^+_2(CO_3)^{2-} \cdot mH_2O$ (A) and structure of $[Zn_3Ga(OH)_8]^+_2[Cu(OH)_4]^{2-} \cdot mH_2O$ as determined by XAFS analyses (B). Interlayer carbonates are not drawn in (A) for clarity.

isotope $^{13}CO_2$ (Cambridge Isotope Laboratories, Inc.; ^{13}C 99%, ^{18}O < 1%) was used.

3. Results

3.1. Copper site structures

The LDH compounds consist of cationic layers with anions such as carbonates and structural water molecules, both in interlayer space (Fig. 1A) [11,29]. For the compound $[Zn_{1.5}Cu_{1.5}Ga(OH)_8]^+_2(CO_3)^{2-} \cdot mH_2O$, Zn, Cu, and Ga cations were in the MO_6 octahedra linked at the edge to form a cationic layer, and the cations distribute statistically [30] to exhibit a similar XANES pattern at the Zn, Cu, and Ga K-edges [11].

The structure of the anions in the LDH compound $[Zn_3Ga(OH)_8]^+_2[Cu(OH)_4]^{2-} \cdot mH_2O$ was studied by Cu K-edge EXAFS [31]. The experimental Fourier transform (FT) (Fig. S1a) was compared to theoretically generated data using FEFF version 8.4 (Fig. S1b–f). As a result, a $(\mu-O)_3Cu(OH)(H_2O)_2$ model accompanied by the coordination of two water molecules (Fig. 1B) [31] was most likely being covalently anchored to cationic layer: $Zn_6Ga_2(OH)_{13}\{(\mu-O)_3Cu(OH)(H_2O)_2\} \cdot mH_2O$ (Supplementary data).

3.2. Rates of photogenerated electron trapping at the Cu sites

Next charge separation in the LDH compounds under $CO_2 + H_2$ and UV–visible light irradiation was monitored by Cu K-edge XANES spectroscopy as the reduction of Cu^{II} sites (Fig. 2). Assuming the wavelength of 354 nm, near the activity maximum as a function of excitation wavelength for the CO_2 photoreduction using LDH [11], the photon number at the sample disk position was on the order of 10 mmol-photons h^{-1} g$_{cat}^{-1}$. A pre-edge peak at 8979 eV because of a 1s–3d transition was used to evaluate the population of Cu^{II} sites [32,33] in the LDH compounds (Fig. 2I). When the electrons separated from holes under UV–visible light diffused to the Cu^{II} sites in the LDH, Cu^{II} sites were reduced to Cu^I. The pre-edge peak does not appear for the Cu^I sites with d^{10} configuration.

The reduction of inlayer sites of Cu^{II} to Cu^I was monitored for the LDH compound $[Zn_{1.5}Cu_{1.5}Ga(OH)_8]^+_2(CO_3)^{2-} \cdot mH_2O$ under CO_2 and H_2 and UV–visible light irradiation. The pre-edge peak intensity for 170 mg of incipient LDH (Cu^{II}: 0.55 mmol) monotonously decreased by 15% within 50 min of irradiation (Fig. 2II-a and III-a). The occurrence of reduction suggests that photogenerated electrons in the LDHs diffused and were trapped at Cu sites. The e$^-$ trapping rate was 580 μmol h^{-1} g$_{cat}^{-1}$ (Table 1A). This rate was lower than reported Cu^{2+} photoreduction rate (2.2 mmol h^{-1} g$_{TiO_2}^{-1}$) in TiO_2 suspension and sacrificial reducing

Table 1

Comparison of the rates of photocatalytic/thermal conversion of CO_2 with those of the elementary step measured by FTIR and Cu K-edge XANES. (A) CO_2(2.1 kPa) and/or H_2 and (B) CO_2(0.20 kPa) or CO_2(0.20 kPa) + H_2(21.7 kPa).

(A)

Photocatalyst	Catalytic rate in CO_2&H_2[a] (μmol h⁻¹ g$_{cat}$⁻¹)			
	Under UV–vis[c]		At 313 K, in dark	
	Methanol formation	CO formation	Methanol formation	CO formation
$[Zn_{1.5}Cu_{1.5}Ga(OH)_8]^+_2(CO_3)^{2-}\cdot mH_2O$	0.31[e]	0.18[e]	<0.0020	<0.0051
$[Zn_3Ga(OH)_8]^+_2[Cu(OH)_4]^{2-}\cdot mH_2O$	0.30	0.13	<0.0020	0.021
$[Zn_{1.5}Cu_{1.5}Ga(OH)_8]^+_2[Cu(OH)_4]^{2-}\cdot mH_2O$	0.49	0.070	0.023	0.0086

Photocatalyst	Elementary step rate (μmol h⁻¹ g$_{cat}$⁻¹)							
	In ¹³CO_2	In vac	In vac, under UV–vis	In H_2,[b] under UV–vis	In ¹³CO_2	In vac, under UV–vis	In ¹³CO_2 and H_2,[b] under UV–vis	In ¹³CO_2 and H_2, light off
	$CO_2 \to HCO_3$ decomposition		Interlayer Cu–OH decrease			Interlayer Cu–OH recover	$Cu^{II} + e^- \to Cu^I$	$Cu^I + h^+ \to Cu^{II}$
$[Zn_{1.5}Cu_{1.5}Ga(OH)_8]^+_2(CO_3)^{2-}\cdot mH_2O$	16[d]	1.3[d]	110[f]	66[f]	180	30[f]	580	1600
$[Zn_3Ga(OH)_8]^+_2[Cu(OH)_4]^{2-}\cdot mH_2O$	400[f]	11[f]				7.7[f]	36	2200
$[Zn_{1.5}Cu_{1.5}Ga(OH)_8]^+_2[Cu(OH)_4]^{2-}\cdot mH_2O$						7.1[f]		

(B)

Photocatalyst	Elementary step rate (μmol h⁻¹ g$_{cat}$⁻¹)				Catalytic rate in CO_2&H_2 (μmol h⁻¹ g$_{cat}$⁻¹)	
	In ¹³CO_2	In vac	In ¹³CO_2	In vac	Under UV–vis Methanol formation	CO formation
	$CO_2 \to HCO_3$	HCO_3 decomposition	Interlayer Cu–OH decrease	Interlayer Cu–OH recover		
$[Zn_3Ga(OH)_8]^+_2[Cu(OH)_4]^{2-}\cdot mH_2O$	32[g]	7.2[g]	15[g]	2.4[g]	0.0027	<0.0051

[a] 21.7 kPa of H_2.
[b] 4.3 kPa of H_2.
[c] From Ref. [12].
[d] Based on peaks at 1647 cm⁻¹.
[e] Preheated at 423 K.
[f] Based on peaks at 1629 and 3673 cm⁻¹.
[g] Based on peak at 1629 and 3664 cm⁻¹.
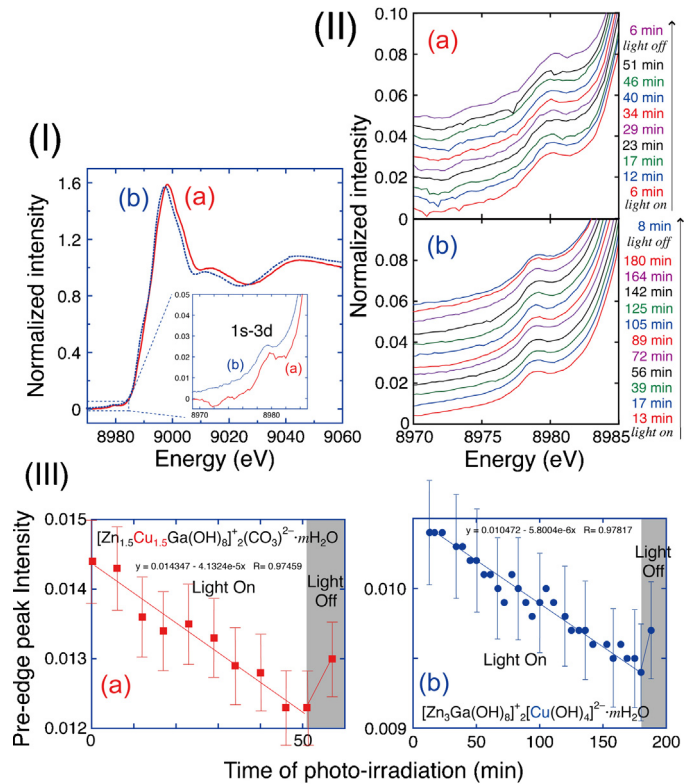
Fig. 2. (I) Normalized Cu K-edge XANES spectra of $[Zn_{1.5}Cu_{1.5}Ga(OH)_8]^+_2(CO_3)^{2-}\cdot mH_2O$ preheated at 423 K (a) and fresh $[Zn_3Ga(OH)_8]^+_2[Cu(OH)_4]^{2-}\cdot mH_2O$ (b) [(Inset) Expanded view of the 1s–3d pre-edge peak region] and (II) under CO_2 (2.1 kPa) + H_2 (21.7 kPa) and UV–visible light irradiation (a: 6–51 min; b: 13–180 min) and subsequent change after the light was turned off (a: 6 min; b: 8 min), and (III) time course of the 1s–3d peak intensity for the two LDH photocatalysts under CO_2 (2.1 kPa) + H_2 (21.7 kPa) and UV–visible light irradiation and subsequent change after the light was turned off. The amount of the LDH photocatalyst charged in the photoreaction cell was 170 mg.

agent $HCO_2^-Na^+$ (0.1 mol L⁻¹) [34], but higher than the Cu^{II} photoreduction rate (4.1 μmol h⁻¹ g$_{cat}$⁻¹) for a Cu–ZnO photocatalyst (0.5 wt% of Cu) in the presence of CO, O_2, and H_2 gas [28].

In total, only 0.38% of the trapped electrons should be available for photocatalytic six – e⁻ reduction to methanol (0.31 μmol h⁻¹ g$_{cat}$⁻¹) and two – e⁻ reduction to CO (0.18 μmol h⁻¹ g$_{cat}$⁻¹) [12] (Table 1A), suggesting the rate of lateral e⁻ diffusion to Cu sites within the cationic layers was sufficient (Fig. 1A) in contrast to that of subsequent e⁻ transfer from Cu sites to substrates/intermediates.

When the UV–visible light was turned off, the Cu^I sites oxidized back to Cu^{II} (Fig. 2II-a and III-a) at a rate of 1600 μmol h⁻¹ g$_{cat}$⁻¹, higher than the e⁻ trap rate (580 μmol h⁻¹ g$_{cat}$⁻¹) at the Cu sites under light (Table 1A).

The 1s–3d pre-edge peak intensity for 170 mg of incipient $[Zn_3Ga(OH)_8]^+_2[Cu(OH)_4]^{2-}\cdot mH_2O$ (Cu^{II}: 0.17 mmol) also monotonously decreased by 11% within 180 min of irradiation (Fig. 2II-b and III-b). In contrast to that of the LDHs consisting of inlayer Cu sites, the reduction rate of Cu^{II} (Fig. 2I-b) to Cu^I at interlayer Cu sites (Fig. 1B) was 36 μmol h⁻¹ g$_{cat}$⁻¹ for $[Zn_3Ga(OH)_8]^+_2[Cu(OH)_4]^{2-}\cdot mH_2O$ (Table 1A). The rate was essentially the slower e⁻ diffusion rate in the perpendicular direction to interlayer Cu sites later than the faster e⁻ diffusion in the cationic layers. Even though the interlayer Cu sites were covalently bonded to O atoms in the cationic layers (Fig. 1B), the e⁻ diffusion rate in the perpendicular direction (36 μmol h⁻¹ g$_{cat}$⁻¹) was smaller than that in the parallel, inlayer direction (580 μmol h⁻¹ g$_{cat}$⁻¹). In total, 5.7% of the trapped electrons were used for photocatalysis to form

methanol ($0.30\,\mu\text{mol h}^{-1}\,\text{g}_{\text{cat}}^{-1}$) and CO ($0.13\,\mu\text{mol h}^{-1}\,\text{g}_{\text{cat}}^{-1}$) [12] (Table 1A). When the UV–visible light was turned off, the Cu$^{\text{I}}$ sites quickly oxidized back to Cu$^{\text{II}}$ (Fig. 2II-b and III-b) at a rate of $2200\,\mu\text{mol h}^{-1}\,\text{g}_{\text{cat}}^{-1}$.

The Zn and Ga K-edge XANES spectra for $[\text{Zn}_{3-x}\text{Cu}_x\text{Ga(OH)}_8]^+_2(\text{CO}_3)^{2-}\cdot m\text{H}_2\text{O}$ were already reported in Ref. [11]. The photogenerated electron trap was only observed in Cu K-edge in situ XANES (Fig. 2) due to the reduction of Cu$^{\text{II}}$ sites to Cu$^{\text{I}}$. However, partially reduced state from Zn$^{\text{II}}$ or Ga$^{\text{III}}$ was not successfully detected in the Zn or Ga K-edge in situ XANES spectra.

3.3. Monitoring carbonate, hydrogen carbonate, and hydroxy species for $[\text{Zn}_3\text{Ga(OH)}_8]^+_2[\text{Cu(OH)}_4]^{2-}\cdot m\text{H}_2\text{O}$

Next, the interactions of $[\text{Zn}_3\text{Ga(OH)}_8]^+_2[\text{Cu(OH)}_4]^{2-}\cdot m\text{H}_2\text{O}$ with CO_2/$^{13}\text{CO}_2$ (2.1–0.20 kPa) were monitored by FTIR at 290 K.

Under CO_2 at 2.1 kPa for 3–62 min, two peaks (1655 and 1570 cm^{-1}) gradually increased, while a sharp peak at 3671 cm^{-1} gradually weakened (Fig. 3A). A weak shoulder peak was also observed at 1511 cm^{-1}. Under $^{13}\text{CO}_2$ at 2.1 kPa for 3–62 min, three overlapping peaks (1629, 1530, and 1474 cm^{-1}) gradually increased and a sharp peak at 3673 cm^{-1} gradually weakened (Figs. 3B and 4B).

If we consider the isotope wavenumber shift based on the harmonic equation [35], the peaks at 1655, 1570, and 1511 cm^{-1} under CO_2 (Fig. 3A) shift to 1618, 1535, and 1477 cm^{-1}, which is consistent with the values observed in $^{13}\text{CO}_2$ (1629, 1530, and 1474 cm^{-1}; Fig. 3B).

For Cu$^{\text{I}}$/TiO$_2$ in CO_2, the peaks at 1663 and 1554 cm^{-1} were assigned to hydrogen carbonate (or carboxylate) and carbonate, respectively [15]. For ZnO in CO_2, the peaks at 1635, 1595–1580, and 1522 cm^{-1} were assigned to hydrogen carbonate, bidentate carbonate, and polydentate carbonate, respectively [36]. For MgO, the peaks at 1685 and 1526 cm^{-1} were assigned to hydrogen carbonate and unidentate carbonate, respectively [37]. Systematic vibration mode assignment of hydrogen carbonate, bidentate carbonate, and polydentate carbonate has been well summarized pictorially [38]. Thus, the peak at 1655 cm^{-1} and the two peaks at 1570 and 1511 cm^{-1} observed for $[\text{Zn}_3\text{Ga(OH)}_8]^+_2[\text{Cu(OH)}_4]^{2-}\cdot m\text{H}_2\text{O}$ in CO_2 (Fig. 3A) were assigned to antisymmetric vibrations of CO$_3$ [$\nu_{\text{as}}(\text{CO}_3)$] of hydrogen carbonate, $\nu_{\text{as}}(\text{CO}_3)$ of bidentate carbonate, and $\nu_{\text{as}}(\text{CO}_3)$ of polydentate carbonate, respectively.

The peak intensity ratio at 1511 cm^{-1} in CO_2 was inconsistent with the corresponding one at 1474 cm^{-1} in $^{13}\text{CO}_2$. This was due to impurity carbonates included in the fresh LDH sample of $[\text{Zn}_3\text{Ga(OH)}_8]^+_2[\text{Cu(OH)}_4]^{2-}\cdot m\text{H}_2\text{O}$. On closer inspection of the as-prepared, 2-h evacuated $[\text{Zn}_3\text{Ga(OH)}_8]^+_2[\text{Cu(OH)}_4]^{2-}\cdot m\text{H}_2\text{O}$ sample, the carbonate peak intensity at 1513 cm^{-1} was 8.0% of that for the same molar amount of the $[\text{Zn}_{1.5}\text{Cu}_{1.5}\text{Ga(OH)}_8]^+_2(\text{CO}_3)^{2-}\cdot m\text{H}_2\text{O}$ disk, indicating that the exact formula was $[\text{Zn}_3\text{Ga(OH)}_8]^+_2[\text{Cu(OH)}_4]^{2-}{}_{0.92}(\text{CO}_3)^{2-}{}_{0.08}\cdot m\text{H}_2\text{O}$. Note that the interlayer anions $[\text{Cu(OH)}_4]^{2-}$ actually existed such as $(\mu\text{–O})_3\text{Cu(OH)(H}_2\text{O})_2$ (Fig. 1B) but were denoted as the species present before dehydration to avoid having a highly complicated composition formula. The impurity should originate from exposure to atmospheric CO_2 (remaining after the 2-h evacuation) during the drying sequence of the LDH synthesis at 290 K.

The amount of impurity carbonate in the LDH sample (4.0 $\mu\text{mol}_{\text{CO}_3}$ per 50 mg$_{\text{LDH}}$) was not negligible vs. the photocatalytic rate on the order of 1–10^2 $\mu\text{mol h}^{-1}$ starting from $\text{CO}_2 + \text{H}_2$ (Table 1). The impurity carbonates interfered with quantitative measurement of carbonate peaks in CO_2. In contrast, new carbonate peaks consisting of ^{13}C could be clearly detected at 1530 and 1474 cm^{-1} in $^{13}\text{CO}_2$. The change of impurity carbonate during pretreatment in vacuum (290 K) affected the FTIR data in CO_2, but the
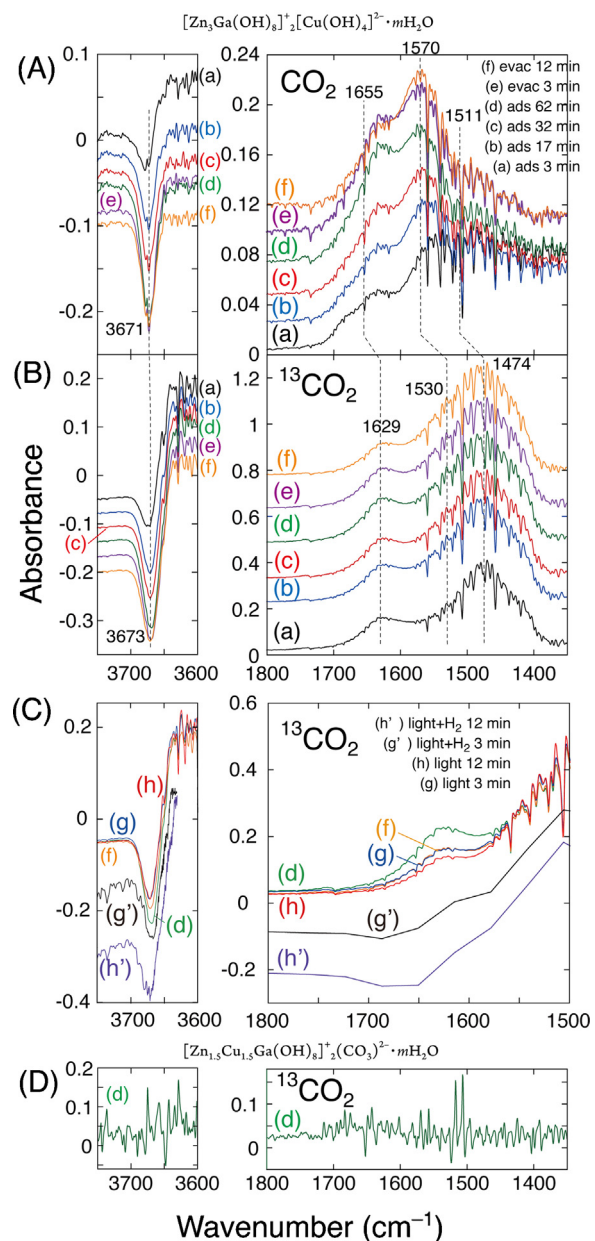
Fig. 3. FTIR spectra for LDH compound $[\text{Zn}_3\text{Ga(OH)}_8]^+_2[\text{Cu(OH)}_4]^{2-}\cdot m\text{H}_2\text{O}$ under CO_2 at 2.1 kPa (A) and under $^{13}\text{CO}_2$ at 2.1 kPa (B and C) for 3 min (a), 17 min (b), 32 min (c), and 62 min (d), evacuated for 3 min (e) and 12 min (f), irradiated by UV–visible light for 3 min (g) and 12 min (h), and under H$_2$ at 4.3 kPa irradiated by UV–visible light for 3 min (g′) and 12 min (h′). FTIR spectra for LDH compound $[\text{Zn}_{1.5}\text{Cu}_{1.5}\text{Ga(OH)}_8]^+_2(\text{CO}_3)^{2-}\cdot m\text{H}_2\text{O}$ under $^{13}\text{CO}_2$ at 2.1 kPa (D) for 62 min (d). The amount of LDH was 50 mg.

exchange between $^{12}\text{CO}_3$ and $^{13}\text{CO}_2$ seems slower than the reactions of $^{13}\text{CO}_2$ with surface. Fortunately in view of catalysis, the 8.0% of carbonate was quite inert in later steps than the pretreatment in vacuum and negligibly affected the photoreduction of CO_2.

The O atom source to form carbonate under CO_2 is unclear. The O atom formed by partial dehydration of hydroxy groups on the cationic layer during pretreatment (290 K, vacuum) is one potential source. Instead, O atom of $(\mu\text{–O})_3\text{Cu(OH)(H}_2\text{O})_2$ species could react with CO_2 to form carbonates.

To evaluate the molar amount of hydrogen carbonate species, CO_2 uptake was volumetrically monitored for the LDH sample after the 2-h evacuation [39]. The CO_2 uptake after 1 h (Fig. 4B) was equalized to the total peak area of hydrogen carbonate and
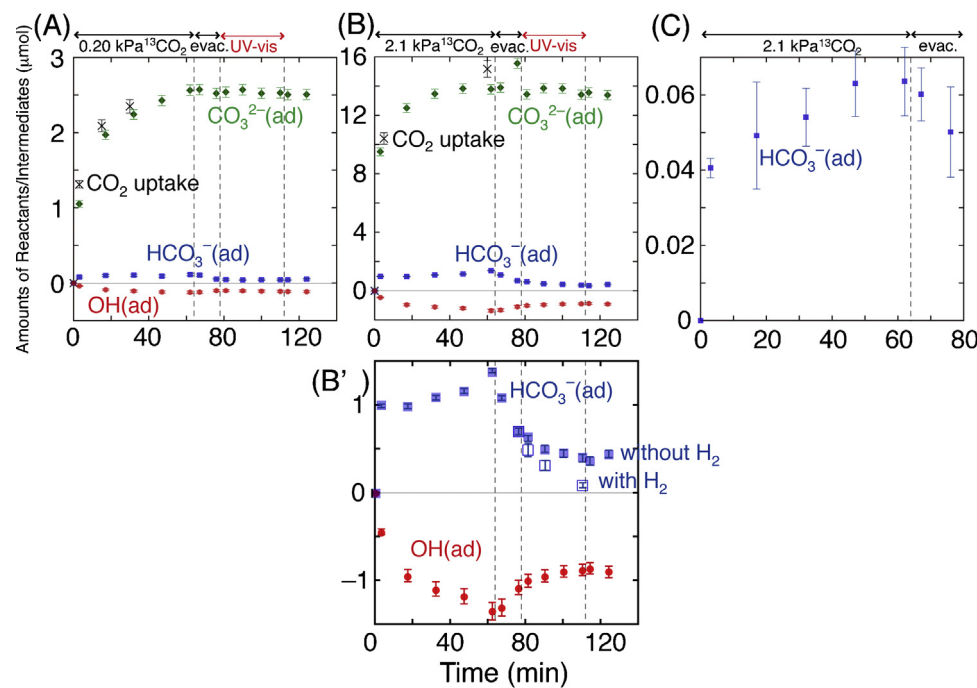
Fig. 4. The amount of $^{13}CO_2$ uptake at 290 K and the increase/decrease of surface hydrogen carbonate (1629–1647 cm^{-1}; ■, square), carbonate (1530, 1474 cm^{-1}; ♦, diamond), and isolated hydroxy (3673 cm^{-1}; ●, circle) species in the FTIR spectra for $[Zn_3Ga(OH)_8]^+_2[Cu(OH)_4]^{2-}\cdot mH_2O$ (50 mg; A and B) and $[Zn_{1.5}Cu_{1.5}Ga(OH)_8]^+_2(CO_3)^{2-}\cdot mH_2O$ (50 mg; C). The $^{13}CO_2$ gas was introduced to the LDH samples at 0.20 kPa (A) or 2.1 kPa (B and C). Panel B′ was expanded from panel B. UV–visible light was irradiated in the absence of H_2 (A and B) and in H_2 at 4.3 kPa (□, open square, B′) at 78–112 min.

carbonate species identified by FTIR. We assumed that the molar absorption coefficients for hydrogen carbonate (1629 cm^{-1}) and carbonates (1530 and 1474 cm^{-1}) were identical. The result of this evaluation of the LDH sample of $[Zn_3Ga(OH)_8]^+_2[Cu(OH)_4]^{2-}\cdot mH_2O$ (0.52 $mmol_{CO_2}$ g_{LDH}^{-1} for 12-h sorption) was in accord with reported CO_2 uptake values (0.5–1.4 mmol g_{LDH}^{-1}) [40,41] and the amount of interlayer Cu sites (0.99 mmol g_{LDH}^{-1}) in the LDH.

In contrast to the stable, inert carbonate peaks, the hydrogen carbonate peak at 1629 cm^{-1} grew at a rate of 400 μmol h^{-1} g_{cat}^{-1} under 2.1 kPa of $^{13}CO_2$ and decomposed at a rate of 110 μmol h^{-1} g_{cat}^{-1} under vacuum (Table 1A and Fig. 4B). The peak under $^{13}CO_2$ for 62 min and under vacuum for 14 min further decreased at the rate of 11 μmol h^{-1} g_{cat}^{-1} during UV–visible irradiation (Figs. 3C-g, C-h and 5B and Table 1A). Alternatively, when H_2 at 4.3 kPa was added before UV–visible irradiation treatment, carbonate peaks still remained constant, while the decrease in the hydrogen carbonate peak was accelerated to 66 μmol h^{-1} g_{cat}^{-1} by hydrogen exposure (Figs. 3C-g′, C-h′ and 4B′ and Table 1A).

The isolated hydroxy peak at 3673 cm^{-1} in $^{13}CO_2$ for $[Zn_3Ga(OH)_8]^+_2[Cu(OH)_4]^{2-}\cdot mH_2O$ (Fig. 3B) was not observed for $[Zn_{1.5}Cu_{1.5}Ga(OH)_8]^+_2(CO_3)^{2-}\cdot mH_2O$ (Fig. 3D). Therefore, it was assigned to OH stretching vibrations [$\nu(OH)$] of $(\mu-O)_3Cu(OH)(H_2O)_2$ species in $[Zn_3Ga(OH)_8]^+_2[Cu(OH)_4]^{2-}\cdot mH_2O$ (Fig. 1B). The peak decrease under $^{13}CO_2$ is plotted in Fig. 4B and B′ (180 μmol h^{-1} g_{cat}^{-1}; Table 1A). In this plot, the decreased molar amount of hydroxy group was assumed to be equal to the molar quantity of hydrogen carbonate formed over 62 min. The hydrogen carbonate peak intensity (1629 cm^{-1}) at 62 min corresponded to 2.8% of that of the $(\mu-O)_3Cu(OH)(H_2O)_2$ site after being transformed to $(\mu-O)_3Cu(O_2C–OH)(H_2O)_2$.

As soon as the gaseous $^{13}CO_2$ was evacuated, the hydroxy peak recovered at the rate of 30 μmol h^{-1} g_{cat}^{-1} (Figs. 3B, 4B and B′ and Table 1A). The decrease/increase of hydroxy group did not coincide with the change observed for hydrogen carbonate, but it did

correlate with 27–45% of the rate increase/decrease of hydrogen carbonate formation.

Then, under UV–visible light irradiation, the peak due to isolated hydroxy groups further recovered at the rate of 7.7 μmol h^{-1} g_{cat}^{-1} (Fig. 3C-g and C-h and Table 1A), similar to the rate of hydrogen carbonate decomposition (11 μmol h^{-1} g_{cat}^{-1}) under this condition. Alternatively, when H_2 at 4.3 kPa was added before the UV–visible irradiation, the recovery of the peak associated with isolated hydroxy group did not change significantly (7.1 μmol h^{-1} g_{cat}^{-1}; Fig. 3C-g′ and C-h′ and Table 1A), suggesting hydrogen carbonate did not totally decompose back to initial CO_2 + surface hydroxy group, but it was further photoreduced by hydrogen.

FTIR monitoring was also performed at a lower pressure of $^{13}CO_2$ (0.20 kPa). The rates of both hydrogen carbonate formation/decomposition and the decrease/recovery of Cu–OH species slowed by an order of magnitude (Table 1B). However, the rates of formation of Cu–OH species were again lower than those for hydrogen carbonate formation by a factor of 47–33% (Table 1B), comparable to the ratios for the test run under $^{13}CO_2$ at 2.1 kPa (Table 1A).

3.4. Monitoring carbonate, hydrogen carbonate, and hydroxy species for $[Zn_{1.5}Cu_{1.5}Ga(OH)_8]^+_2(CO_3)^{2-}\cdot mH_2O$

For $[Zn_{1.5}Cu_{1.5}Ga(OH)_8]^+_2(CO_3)^{2-}\cdot mH_2O$ under 2.1 kPa of $^{13}CO_2$, the signals from interlayer carbonate interfered with those of the additional minor carbonate and/or hydrogen carbonate and the spectra were less precise compared to those for $[Zn_3Ga(OH)_8]^+_2[Cu(OH)_4]^{2-}\cdot mH_2O$ (Fig. 3D). A broad peak at 1647 cm^{-1} increased at the rate of 16 μmol h^{-1} g_{cat}^{-1} under $^{13}CO_2$ and decreased at the rate of 1.3 μmol h^{-1} g_{cat}^{-1} under vacuum (Fig. 4C). This peak can be assigned to hydrogen carbonate and quantified using the same criteria as that in Fig. 3B. The molar amount of hydrogen carbonate under $^{13}CO_2$ exposure after 62 min corresponded to 0.12% of that of carbonate anion in the LDH
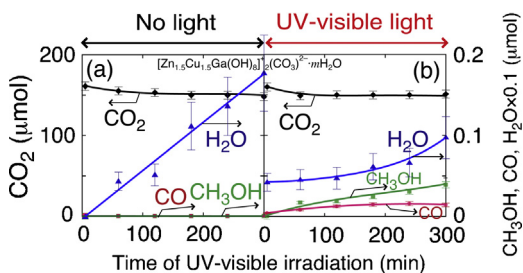
**Fig. 5.** Time course of the photocatalytic reaction under CO_2 (2.3 kPa) + H_2 (21.7 kPa). The amount of LDH photocatalysts $[Zn_{1.5}Cu_{1.5}Ga(OH)_8]^+_2(CO_3)^{2-}\cdot mH_2O$ was 100 mg. The reactor was set at 313 K in the dark (a) or below 313 K under UV–visible light from a Xe arc lamp (b). CO_2 (♦, diamond), H_2O (▲, triangle), CH_3OH (■, square), and CO (●, circle).

compound. In the ν(OH) region, no peak due to isolated hydroxy group appeared (Fig. 3D, left).

3.5. CO₂ conversion tests under light and in the dark at 313 K

Hydrogen carbonate observed in the FTIR spectra under CO_2 can be reduced by the electrons trapped at the Cu site, as monitored by XANES. CO was formed (0.13 μmol h^{-1} g$_{cat}$$^{-1}$) using $[Zn_3Ga(OH)_8]^+_2[Cu(OH)_4]^{2-}\cdot mH_2O$ [12] as resulting from the reaction of a reduced hydrogen carbonate with a proton and an e$^-$ to form CO and water at the interlayer sites including the Cu sites [11]. On the other hand, methanol formation (0.30 μmol h^{-1} g$_{cat}$$^{-1}$) from a reduced hydrogen carbonate still requires multiple reduction steps. To obtain insight into the steps, kinetic tests under UV–visible light, and control tests in the dark at 313 K (maximum accessible temperature at the reactor under the test conditions [11]) were performed under CO_2 and H_2 using $[Zn_{1.5}Cu_{1.5}Ga(OH)_8]^+_2(CO_3)^{2-}\cdot mH_2O$.

No products above the detection limit of GC–TCD were detected over a 5-h period in the dark at 313 K using $[Zn_{1.5}Cu_{1.5}Ga(OH)_8]^+_2(CO_3)^{2-}\cdot mH_2O$ (Table 1A and Fig. 5a). When UV–visible light was applied, the reactor was below 313 K, and a major amount of methanol and minor amount of CO were formed (Fig. 5b). Thus, hydrogen carbonate, which formed bound to inlayer Cu ions (Fig. 1A), should be reduced by multiple e$^-$ transfer via the forbidden direct e$^-$ transition from O 2p to M 3d (M = Zn, Cu, or Ga) in LDHs [11,12] and H$^+$ transfer.

By contrast, in the dark at 313 K using $[Zn_3Ga(OH)_8]^+_2[Cu(OH)_4]^{2-}\cdot mH_2O$, CO was formed at the rate of 21 nmol h^{-1} g$_{cat}$$^{-1}$, but no methanol was found (Table 1A). The rate was 16% of that observed under UV–visible light [12]. Using $[Zn_{1.5}Cu_{1.5}Ga(OH)_8]^+_2[Cu(OH)_4]^{2-}\cdot mH_2O$, trace amounts of methanol and CO formed at the rates of 23 and 8.6 nmol h^{-1} g$_{cat}$$^{-1}$, respectively (Table 1A). The rates were 4.7% and 12%, respectively, of those observed under UV–visible light [12].

In addition, a photocatalytic test under CO_2 at 0.20 kPa + H_2 at 21.7 kPa was performed for comparison to the reported results under CO_2 at 2.1 kPa + H_2 at 21.7 kPa (Table 1A) [12] using $[Zn_3Ga(OH)_8]^+_2[Cu(OH)_4]^{2-}\cdot mH_2O$. The methanol and CO formation rates were only 0.90% and less than 3.9%, respectively, of those under CO_2 at 2.1 kPa (Table 1B).

4. Discussion

4.1. Photogenerated electron trap

The Cu K-edge EXAFS analysis (Supplementary data) indicated that the structure of the interlayer Cu sites for the LDH compound $[Zn_3Ga(OH)_8]^+_2[Cu(OH)_4]^{2-}\cdot mH_2O$ transformed into $(\mu-O)_3Cu(OH)(H_2O)_2$ by reaction with hydroxy

groups in the cationic layer (Fig. 1B). As determined by Cu K-edge in situ XANES monitoring, electron trapping (580 μmol h^{-1} g$_{cat}$$^{-1}$) at the Cu sites was 18–260 times faster than that observed for catalytic CO_2 conversion into methanol + CO using $[Zn_{1.5}Cu_{1.5}Ga(OH)_8]^+_2(CO_3)^{2-}\cdot mH_2O$ (2.2 μmol-e$^-$ h^{-1} g$_{cat}$$^{-1}$) and $[Zn_3Ga(OH)_8]^+_2[Cu(OH)_4]^{2-}\cdot mH_2O$ (2.1 μmol-e$^-$ h^{-1} g$_{cat}$$^{-1}$) under light (Table 1A). Furthermore, e$^-$ trapping was 16 times faster for inlayer Cu sites in $[Zn_{1.5}Cu_{1.5}Ga(OH)_8]^+$ than for interlayer Cu sites as anchored $(\mu-O)_3Cu(OH)(H_2O)_2$ (36 μmol h^{-1} g$_{cat}$$^{-1}$; Table 1A).

In summary, photogenerated e$^-$ trapping at the Cu sites of LDH samples in this study was fast enough compared to photocatalysis to afford CO_2 conversion. Specifically, lateral e$^-$ diffusion in the cationic sheets (Fig. 1A) was faster than diffusion in the direction perpendicular to the attached $(\mu-O)_3Cu(OH)(H_2O)_2$ sites (Fig. 1B).

4.2. Dynamic equilibrium of CO₂ with hydrogen carbonate

In the FTIR measurements of $[Zn_3Ga(OH)_8]^+_2[Cu(OH)_4]^{2-}\cdot mH_2O$ under $^{13}CO_2$, carbonate $\nu_{as}(CO_3)$ peaks were observed at 1530 and 1474 cm^{-1} (Fig. 3B). The peaks were stable in vacuum or an atmosphere of H_2 and/or under irradiation with UV–visible light, suggesting bidentate/polydentate carbonate species were not incorporated during catalytic CO_2 reduction under UV–visible light.

By contrast, for the LDHs, the hydrogen carbonate $\nu_{as}(CO_3)$ peak was weaker (1629 cm^{-1} under $^{13}CO_2$, Fig. 3B) and the species were in equilibrium with CO_2 and hydroxy groups. The rates of increase and decrease of the hydrogen carbonate peak under $^{13}CO_2$ and vacuum (Fig. 3B) were 400 and 110 μmol h^{-1} g$_{cat}$$^{-1}$, 930- and 260-fold higher, respectively, than those of catalytic CO_2 conversion and slightly greater than the e$^-$ trapping rates at the Cu sites (Table 1A). In this case, CO_2 is in equilibrium with hydroxy groups in the cation layers or interlayer $(\mu-O)_3Cu(OH)(H_2O)_2$ species.

$$CO_2 + HO(\text{cationic layer}) \rightleftarrows HO-CO_2(\text{cationic layer})$$

$$CO_2 + (\mu-O)_3Cu(OH)(H_2O)_2 \rightleftarrows (\mu-O)_3Cu(O_2C-OH)(H_2O)_2$$

The equilibrium of CO_2 with Zn–OH sites to form hydrogen carbonate was calculated on the basis of Hartree–Fock and DFT to be exothermic by 33 kJ mol^{-1} [42]. As in Ref. [42], hydrogen carbonate species in this study may also form hydrogen bonds with neighboring hydroxy groups. The equilibrium of CO_2 (and water) with $Cu_2O(111)$ surface species, as observed by DFT calculations, was also reported. Hydrogen carbonate was the major surface species and was suggested as the intermediate in the reduction of CO_2 [43].

All the LDH compounds in this study were precipitated at pH 8 during the synthesis and have a basic nature. Near the basic surface in the interlayer space of the LDHs [44], the following equilibrium is also plausible.

$$CO_2 + H_2O(\text{interlayer}) \rightleftarrows HO-CO^{2-}(\text{interlayer}) + H^+(\text{interlayer})$$
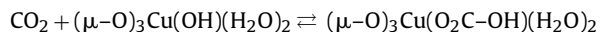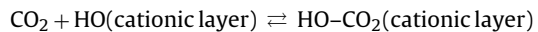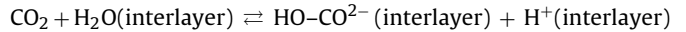
The sharp peaks that appeared at 3671–3673 cm^{-1} in CO_2 (Fig. 3A) or $^{13}CO_2$ (Panel B) were assigned to ν_{OH} for interlayer hydroxy group at $(\mu-O)_3Cu(OH)(H_2O)_2$ sites (Fig. 1B). These were separated from the ν_{OH} peaks of interlayer water molecules (3348 cm^{-1}) and those of hydroxy groups in the cationic layers (3468 cm^{-1}) [45]. The rates of decrease and increase of the hydroxy peak were not equivalent to the rates of increase and decrease of the hydrogen carbonate peak in $^{13}CO_2$; rather, the latter rates were greater by 2.2–3.7-fold. The situation was similar when a lower pressure (0.20 kPa) of $^{13}CO_2$ was used (2.1–3.0-fold).

In summary, the hydroxy groups of the cationic layers and/or interlayer water reacted in the early stage of $^{13}CO_2$ exposure, and
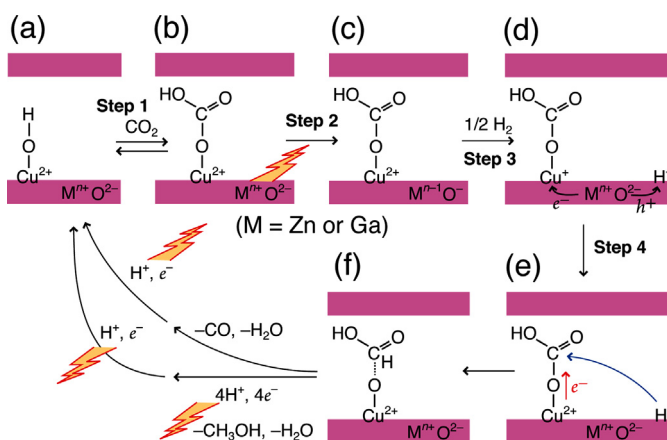
Scheme 1. Proposed photocatalytic cycle of CO_2 reduction to methanol or CO using LDH catalysts consisting of Zn, Ga, and interlayer Cu sites.

the slower diffusion of CO_2 into the interlayer space later led to the formation of $(\mu\text{-}O)_3Cu(O_2C\text{-}OH)(H_2O)_2$. If the isolated hydroxy peak was because of an impurity (e.g., $Cu(OH)_2$) powder that coexisted with $[Zn_3Ga(OH)_8]^+_2[Cu(OH)_4]^{2-}\cdot mH_2O)$ [12], this time delay cannot be rationalized.

Hydrogen carbonate formation was difficult to monitor for $[Zn_{1.5}Cu_{1.5}Ga(OH)_8]^+_2(CO_3)^{2-}\cdot mH_2O$ under CO_2 or $^{13}CO_2$ owing to the strong IR absorption of the enormous amount of interlayer carbonates. Even so, the rates of formation and decomposition (16–1.3 μmol h^{-1} g_{cat}^{-1}; Table 1A) were significantly lower (4.0–1.2% of those for $[Zn_3Ga(OH)_8]^+_2[Cu(OH)_4]^{2-}\cdot mH_2O$). The smaller interlayer spacing for $[Zn_{1.5}Cu_{1.5}Ga(OH)_8]^+_2(CO_3)^{2-}\cdot mH_2O$ compared to that for $[Zn_3Ga(OH)_8]^+_2[Cu(OH)_4]^{2-}\cdot mH_2O$ (0.753 nm [11] vs. 0.792 nm [12]) may be the reason.

The hydrogen carbonate peaks at 1629 cm^{-1} for $[Zn_3Ga(OH)_8]^+_2[Cu(OH)_4]^{2-}\cdot mH_2O$ increased under $^{13}CO_2$ at 2.1 kPa and quickly decreased under vacuum or UV–visible light (Fig. 4B and B′). The peak decrease under UV–visible light was further accelerated 6.0-fold in the presence of H_2 (Fig. 4B′). In clear contrast, the recovery of the isolated Cu–OH peak was not affected by the presence of H_2 (7.7 and 7.1 μmol h^{-1} g_{cat}^{-1}, Fig. 3C and Table 1A). This difference suggested that hydrogen carbonate dominantly decomposed back to initial CO_2 + surface hydroxy under vacuum but was further reduced under H_2 and UV–visible light irradiation (Scheme 1).

The trend in the FTIR measurements under CO_2 and vacuum was similar to that under $^{13}CO_2$ at 0.20 kPa (Fig. 4A). As the amount of hydrogen carbonate in equilibrium decreased (from 28 to 2.3 μmol g_{cat}^{-1}), the rates of formation/decomposition were reduced by an order of magnitude by decreasing the $^{13}CO_2$ pressure from 2.1 to 0.20 kPa (Table 1A and B).

For $[Zn_3Ga(OH)_8]^+_2[Cu(OH)_4]^{2-}\cdot mH_2O$ under CO_2 at 0.20 kPa + H_2 at 21.7 kPa and UV–visible light, the photocatalytic rates of methanol and CO formation decreased by two orders of magnitude (Table 1A and B). Furthermore, when H_2 at 21.7 kPa was introduced to the LDH sample treated with CO_2 for 62 min followed by a 14-min evacuation and the sample was irradiated, methanol formation was confirmed by GC-TCD in addition to CO_2 and CO formation [11].

In summary, the rapid decomposition of the hydrogen carbonate species under vacuum and UV–visible light and its further promotion by the addition of H_2 as well as the critical catalytic rate dependence on the equilibrium concentration of the hydrogen carbonate species strongly suggested that hydrogen carbonate was the intermediate in the photocatalytic formation of methanol and CO from CO_2 using the LDH compounds.

4.3. Photocatalytic reaction mechanism from CO_2

On the basis of our study by Cu K-edge in situ XANES and in situ FTIR, we postulate the following initial reaction steps for the CO_2 photoreduction at the LDH interlayer sites including the interlayer Cu sites (Scheme 1): (Step 1) the reaction of CO_2 with hydroxy group bound to interlayer Cu^{II} to form hydrogen carbonate, (Step 2) the forbidden direct e^- transition from O 2p to M 3d (M = Zn, Ga) [11], (Step 3) the diffusion of electrons and holes in the LDHs to Cu^{II} sites and H atom, respectively, at the surface, and (Step 4) the transfer of trapped electrons from Cu^I to hydrogen carbonate forming anionic hydrogen carbonate. Steps 1 and 2 occurred at a sufficient rate (Table 1), and Step 4 (or possibly an event later than Step 4) should be rate-determining.

The direct e^- transition of LDHs in this study was considered as forbidden, based on the fit [11,12] of UV–visible absorption data to the equation of Davis and Mott. This is forbidden due to the symmetry of the Bloch functions of valence band and conduction band. Even so, minor term in the perturbation Hamiltonian does not diminish due to the symmetry, and weaker absorption was observed experimentally [46].

In this study, no C-containing intermediate/adsorbed species was observed in the FTIR spectra except for carbonates and hydrogen carbonate (Fig. 3), and the bidentate and polydentate carbonates were inert. For TiO_2, the photooxidation of carbonate to CO_3^- radicals was detected by ESR at 4.5 K, but the photocatalytic reaction mechanism was proposed to proceed via a formate species $[CO_2 + H^+ + 2e^- \rightarrow HCO_2^-$ (surface)] followed by conversion to methane [47]. The surface concentration of hydroxy groups was 1.7–4.5 groups nm^{-1} over TiO_2 vs. 1.7×10^5 groups nm^{-1} for $[Zn_{1.5}Cu_{1.5}Ga(OH)_8]^+_2(CO_3)^{2-}\cdot mH_2O$ (specific surface area, 57 m^2 g^{-1}) [11]. Because of this difference, hydrogen carbonate was preferentially observed for the LDH compounds in this study.

Although the e^- diffusion rate to Cu^{II} sites (Step 3) was 16 times greater for $[Zn_{1.5}Cu_{1.5}Ga(OH)_8]^+_2(CO_3)^{2-}\cdot mH_2O$ than for $[Zn_3Ga(OH)_8]^+_2[Cu(OH)_4]^{2-}\cdot mH_2O$ as determined by Cu K-edge in situ XANES (Fig. 2 and Table 1A), the molar ratio of hydrogen carbonate species in $^{13}CO_2$ for 62 min was 0.12% and 2.8%, respectively, to the anion $\{(CO_3)^{2-}$ or $[Cu(OH)_4]^{2-}\}$ of LDHs. In addition to hydrogen carbonate population (23 times greater for $[Zn_3Ga(OH)_8]^+_2[Cu(OH)_4]^{2-}\cdot mH_2O$) effects, e^- transfer at the interface (Step 4) may be more effective between a Cu atom and hydrogen carbonate species $(\mu\text{-}O)_3Cu(O_2C\text{-}OH)(H_2O)_2$ formed at the interlayer Cu–OH sites (Fig. 1B) than between a Cu atom and the hydrogen carbonate species formed at inlayer $(M-)_3OH$ sites (M = Cu, Zn, or Ga; Fig. 1A). By these effects, with $[Zn_3Ga(OH)_8]^+_2[Cu(OH)_4]^{2-}\cdot mH_2O$, a significant improvement in the utilization efficiency of trapped electrons at the Cu sites is observed (5.7% vs. 0.38% at inlayer $(M-)_3OH$ sites). Because of the compensating effects of Steps 3 and 4, the photocatalytic CO_2 conversion rates into methanol and CO were similar for $[Zn_{1.5}Cu_{1.5}Ga(OH)_8]^+_2(CO_3)^{2-}\cdot mH_2O$ [0.49 μmol(CO_2) h^{-1} g_{cat}^{-1}] and $[Zn_3Ga(OH)_8]^+_2[Cu(OH)_4]^{2-}\cdot mH_2O$ [0.43 μmol(CO_2) h^{-1} g_{cat}^{-1}; Table 1A].

4.4. Verification of photocatalysis from $CO_2 + H_2$ using LDHs

Using the LDH compound $[Zn_{1.5}Cu_{1.5}Ga(OH)_8]^+_2(CO_3)^{2-}\cdot mH_2O$, no products were detected after 5 h at 313 K in the dark under CO_2 and H_2 (Fig. 5a). The Zn–Cu–Al LDH was reported to be stable as high as at 573 K [48].

Unfortunately, the purity of $[Zn_{3-x}Cu_xGa(OH)_8]^+_2[Cu(OH)_4]^{2-}\cdot mH_2O$ $(x = 0, 1.5)$ was lower than that of $[Zn_{1.5}Cu_{1.5}Ga(OH)_8]^+_2(CO_3)^{2-}\cdot mH_2O$ in this study; minor CuO and $Cu(OH)_2$ were included for the LDH compounds

$[Zn_{3-x}Cu_xGa(OH)_8]^+_2[Cu(OH)_4]^{2-}\cdot mH_2O$ ($x = 0$, 1.5) [12,31]. In the time course at 313 K using them in the dark, minor CO/methanol were formed later than the induction period of 1–2 h (Table 1A). As one of the plausible reasons, reduced Cu^I sites [49,50] from the Cu^{II} impurity during the induction period may form CO/methanol similar to the process of conventional methanol synthesis [51–53].

5. Conclusions

For the LDH $[Zn_3Ga(OH)_8]^+_2[Cu(OH)_4]^{2-}\cdot mH_2O$, photogenerated e^- diffusion from the bulk to the interlayer $(\mu{-}O)_3Cu(OH)(H_2O)_2$ sites was monitored by Cu K-edge in situ XANES and compared with that of $[Zn_{1.5}Cu_{1.5}Ga(OH)_8]^+_2(CO_3)^{2-}\cdot mH_2O$. The rate of e^- diffusion was 16 times faster for inlayer Cu sites of $[Zn_{1.5}Cu_{1.5}Ga(OH)_8]^+$ than for interlayer $(\mu{-}O)_3Cu(OH)(H_2O)_2$ sites.

The reaction with CO_2 was monitored by in situ FTIR. Hydrogen carbonate (1629 cm^{-1}) was formed under $^{13}CO_2$ at the rate of 400 μmol h^{-1} g$_{cat}^{-1}$, and it decomposed under vacuum at the rate of 110 μmol h^{-1} g$_{cat}^{-1}$ for $[Zn_3Ga(OH)_8]^+_2[Cu(OH)_4]^{2-}\cdot mH_2O$. The peak intensity change was synchronized with the decrease/increase (180–30 μmol h^{-1} g$_{cat}^{-1}$) of an isolated Cu–OH peak (3673 cm^{-1}). The time delay was considered to be due to the diffusion of CO_2 in the interlayer space of LDHs; CO_2 first reacted with hydroxy group in the cationic layers and/or interlayer water and then diffused to react with $(\mu{-}O)_3Cu(OH)(H_2O)_2$ to form $(\mu{-}O)_3Cu(O_2C{-}OH)(H_2O)_2$. For the formation/decomposition of the hydrogen carbonate species, the reactivity of $[Zn_3Ga(OH)_8]^+_2[Cu(OH)_4]^{2-}\cdot mH_2O$ was 25–85 times greater than that of $[Zn_{1.5}Cu_{1.5}Ga(OH)_8]^+_2(CO_3)^{2-}\cdot mH_2O$, possibly due to differences in the interlayer spacing (0.792 vs. 0.753 nm).

The decomposition of hydrogen carbonate proceeded under UV–visible light, and for $[Zn_3Ga(OH)_8]^+_2[Cu(OH)_4]^{2-}\cdot mH_2O$, it was enhanced 6-fold by the addition of H_2. The rate of recovery of the Cu–OH peak changed only negligibly in the presence of H_2 under UV–visible irradiation, suggesting further photoreduction of hydrogen carbonate by H_2. Furthermore, by decreasing the CO_2 pressure, the rates of formation/decomposition of hydrogen carbonate and the rates of photocatalyzed methanol + CO formation from $CO_2 + H_2$ decreased by one to two orders of magnitude, respectively. Thus, hydrogen carbonate was confirmed to be an intermediate in the photocatalysis of CO_2 to methanol and CO.

The LDH compound with the formula $[Zn_{1.5}Cu_{1.5}Ga(OH)_8]^+_2(CO_3)^{2-}\cdot mH_2O$ was synthesized with adequate purity, and no products were detected in the control reaction under $CO_2 + H_2$ at 313 K in the dark. The action of the LDH compounds was confirmed to originate from initial charge separation caused by photons in the photocatalysis under $CO_2 + H_2$.

Appendix A. Supplementary data

Supplementary data associated with this article can be found, in the online version, at http://dx.doi.org/10.1016/j.apcatb.2013.07.065.

References

[1] B.E. Logan, K. Rabaey, Science 337 (2012) 686.
[2] J.F. Hull, Y. Hiomeda, W.H. Wang, B. Hashiguchi, R. Periana, D.J. Szalda, J.T. Muckerman, E. Fujita, Nat. Chem. 4 (2012) 383.
[3] A.J. Morris, G.J. Meyer, E. Fujita, Acc. Chem. Res. 42 (2009) 1983.
[4] R.F. Service, Science 334 (2011) 922.
[5] W.C. Chueh, C. Falter, M. Abbott, D. Scipio, P. Furler, S.M. Haile, A. Steinfeld, Science 330 (2010) 1797.
[6] G.P. Smestad, A. Steinfeld, Ind. Eng. Chem. Res. 51 (2012) 11828.
[7] M. Grätzel, Nature 414 (2001) 338.
[8] Y. Izumi, Coord. Chem. Rev. 257 (2013) 171.
[9] S.C. Roy, O.K. Varghese, M. Paulose, C.A. Grimes, ACS Nano 4 (2010) 1259.
[10] V.P. Indrakanti, J.D. Kubicki, H.H. Schobert, Energy Environ. Sci. 2 (2009) 745.
[11] N. Ahmed, Y. Shibata, T. Taniguchi, Y. Izumi, J. Catal. 279 (2011) 123.
[12] N. Ahmed, M. Morikawa, Y. Izumi, Catal. Today 185 (2012) 263.
[13] K. Teramura, S. Iguchi, Y. Mizuno, T. Shishido, T. Tanaka, Angew. Chem. Int. Ed. 51 (2012) 8008.
[14] M. Morikawa, N. Ahmed, Y. Ogura, Y. Izumi, Appl. Catal. B 117/118 (2012) 317.
[15] C.C. Yang, Y.H. Yu, B. van der Linden, J.C.S. Wu, G. Mul, J. Am. Chem. Soc. 132 (2010) 8398.
[16] T. Yui, A. Kan, C. Saitoh, K. Koike, T. Ibusuki, O. Ishitani, Appl. Mater. Interfaces 3 (2011) 2594.
[17] S. Kaneco, H. Kurimoto, Y. Shimizu, K. Ohta, T. Mizuno, Energy 24 (1999) 21.
[18] S. Kaneco, H. Kurimoto, K. Ohta, T. Mizuno, A. Saji, J. Photochem. Photobiol. A 109 (1997) 59.
[19] M. Anpo, H. Yamashita, Y. Ichihashi, S. Ehara, J. Electroanal. Chem. 396 (1995) 21.
[20] I.A. Shkrob, T.W. Marin, H. He, P. Zapol, J. Phys. Chem. C 116 (2012) 9450.
[21] T. Inoue, A. Fujishima, K. Konishi, K. Honda, Nature 277 (1979) 637.
[22] Y. Izumi, T. Itoi, S. Peng, K. Oka, Y. Shibata, J. Phys. Chem. C 113 (2009) 6706.
[23] The light intensity was measured using a spectroradiometer Model USR–40D (Ushio). The xenon arc lamp irradiated in a wide spectrum between 200 and 1100 nm.
[24] Y. Izumi, F. Kiyotaki, H. Nagamori, T. Minato, J. Electr. Spectrosc. Relat. Phenom. 119 (2001) 193.
[25] Y. Izumi, K. Konishi, D. Obaid, T. Miyajima, H. Yoshitake, Anal. Chem. 79 (2007) 6933.
[26] Y. Izumi, H. Nagamori, F. Kiyotaki, D. Masih, T. Minato, E. Roisin, J.P. Candy, H. Tanida, T. Uruga, Anal. Chem. 77 (2005) 6969.
[27] L. Ankudinov, B. Ravel, J.J. Rehr, S.D. Condradson, Phys. Rev. B 58 (1998) 7565.
[28] Y. Yoshida, Y. Mitani, T. Itoi, Y. Izumi, J. Catal. 287 (2012) 190.
[29] F. Cavani, F. Trifirò, A. Vaccari, Catal. Today 11 (1991) 173.
[30] P.J. Sideris, U.G. Nielsen, Z. Gan, C.P. Grey, Science 321 (2008) 113.
[31] N. Ahmed, M. Morikawa, Y. Izumi, in: S.L. Suib (Ed.), Activation of Carbon Dioxide, Elsevier, 2013, pp. 589–602 (Chapter 20), doi:10.1016/B978-0-444-53882-6.00021-8.
[32] I.J. Pickering, G.N. George, Inorg. Chem. 34 (1995) 3142.
[33] Y. Izumi, H. Nagamori, Bull. Chem. Soc. Jpn. 73 (2000) 1581.
[34] S. Yamazaki, S. Iwai, J. Yano, H. Taniguchi, J. Phys. Chem. A 105 (2001) 11285.
[35] Wavenumber $\tilde{v} = 1/2\pi c(\sqrt{k/\mu})$ was based on harmonic equation in which c is the speed of light, k is the force constant, and reduced mass μ satisfies $1/\mu = 1/M_1 + 1/M_2$. Thus, $\tilde{v}_{13CO}/\tilde{v}_{12CO} = \sqrt{((13+16)/(13\times16))/(12+16)/(12\times16)} = 0.97778$ and $\tilde{v}_{13CH}/\tilde{v}_{12CH} = \sqrt{((13+1)/(13\times1))/((12+1)/(12\times1))} = 0.99704$.
[36] J. Saussey, J.C. Lavalley, C. Bovet, J. Chem. Soc. Faraday Trans. I 78 (1982) 1457.
[37] K. Teramura, T. Tanaka, H. Ishikawa, Y. Kohno, T. Funabiki, J. Phys. Chem. B 108 (2004) 346.
[38] S.E. Collins, M.A. Baltanas, A.L. Bonivardi, J. Catal. 226 (2004) 410.
[39] The CO_2 uptake was measured using a capacitance manometer (ULVAC, Models CCMT–1000A and GM–2001).
[40] C.T. Yavuz, B.D. Shinall, A.V. Iretskii, M.G. White, T. Golden, M. Atilhan, P.C. Ford, G.D. Stucky, Chem. Mater. 21 (2009) 3473.
[41] Z. Yong, A.E. Rodrigues, Ener. Conv. Manage. 43 (2002) 1865.
[42] M. Bräuer, J.L. Pérez-Lustres, J. Weston, E. Anders, Inorg. Chem. 41 (2002) 1454.
[43] H. Wu, N. Zhang, Z. Cao, H. Wang, S. Hong, Int. J. Quantum Chem. 112 (2012) 2532.
[44] Y. Izumi, F. Kiyotaki, T. Minato, Y. Seida, Anal. Chem. 74 (2002) 3819.
[45] J.T. Kloprogge, L. Hickey, R.L. Frost, J. Solid Chem. 177 (2004) 4047.
[46] F. Wooten, Optical Properties of Solids, Academic Press, New York, USA, 1972, 142.

[47] N.M. Dimitrijevic, B.K. Vijayan, O.G. Poluektov, T. Rajh, K.A. Gray, H. He, P. Zapol, J. Am. Chem. Soc. 133 (2011) 3964.
[48] M. Behrens, I. Kasatkin, S. Kühl, G. Weinberg, Chem. Mater. 22 (2010) 386.
[49] S. Poulston, P.M. Parlett, P. Stone, M. Bowker, Surf. Interf. Anal. 24 (1996) 811.
[50] J.Y. Kim, J.A. Rodriguez, J.C. Hanson, A.I. Frenkel, P.L. Lee, J. Am. Chem. Soc. 125 (2003) 10684.
[51] L.C. Grabow, M. Mavrikakis, ACS Catal. 1 (2011) 365.
[52] K. Klier, Adv. Catal. 31 (1982) 243.
[53] S. Fujita, M. Usui, H. Ito, N. Takezawa, J. Catal. 157 (1995) 403.